

# PASSIVELY DRIVEN X-BAND STRUCTURES

T. Sipahi, N. Sipahi, S. G. Biedron, S. V. Milton, CSU, Fort Collins, Colorado, USA

## Abstract

Accelerating structures operated at X-band frequencies have been shown to regularly achieve gradients of around 100 MV/m or better. Obviously, use of such technology can lead to more compact particle accelerators. At the Colorado State University Accelerator Laboratory (CSUAL) we would like to adapt this technology to our L-band (1.3 GHz) accelerator system via a 2-beam configuration that capitalizes on the high gradients achievable in X-band accelerating structures in order to increase our overall beam energy in a manner that does not require investment in an expensive, custom, high-power X-band klystron system. Here we provide the design details of the X-band accelerator structures that will allow us to achieve our goal of reaching the maximum practical net potential across the X-band accelerating structure.

## GENERAL CONCEPT

The CSUAL linac is an L-band system capable of generating 6-MeV electron bunches [1]. The parameters of L-band linac system are given in Table 1. For many reasons we would like to further increase the electron beam energy without additional significant investment. Our idea is to utilize the electron beam from our linac as a drive source for an otherwise unpowered (passive) X-band linac structure, thus allowing us to increase the beam energy by using the L-band power together with the inherent high shunt impedance of the X-band structure. In our previous study [2] we showed that by using a passive standing wave (SW) X-band cavity driven by our linac we had the potential to increase our 6-MeV electron bunch energy to 11 MeV in 15 cm, but there was a fundamental limit of that configuration. Here we utilize a two-beam configuration based on two traveling wave (TW) X-band structures, one used as an X-band power generator (the decelerator), and one as an accelerator. This configuration is shown in Figure 1. We exploit the TW structure's ability to provide continuous X-band power generated from the passing of the L-band system beam through it and then transfer this power to a second cavity that can be filled in a manner that does not limit as before the achievable integrated potential.

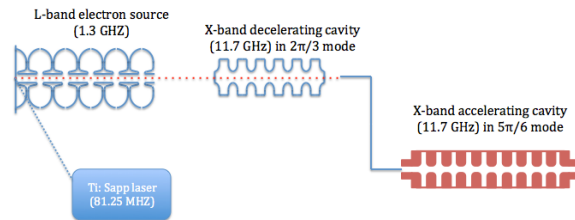


Figure 1: General layout of the two-beam X-band cavity structures [3].

Table 1: Parameters of CSU Accelerator Laboratory

Laser Frequency	81.25 MHz
L-Band RF Gun Frequency	1.3 GHz
L-Band RF Gun Energy	6 MeV
L-Band Macropulse Length	10 $\mu$ s
X-band Linac Frequency	11.7 GHz
Repetition Rate	10 Hz
RF gun Charge/Bunch	3.5 nC

## CAVITY CHOICE

### General

We must design two separate cavities, one to be used as a decelerator and optimized to efficiently generate and allow extraction of X-band power without significant disruption to the passing beam, and the other optimized to efficiently accept X-band power and generate the highest practical integrated potential to be used for accelerating electron bunches.

We use a consistent description of cavity geometries as shown in Figure 2 where  $a$  is the iris radius,  $R$  is the cavity radius,  $h(=2r_1)$  is the disc thickness,  $l$  is the basic cell length,  $\lambda$  is the wavelength and  $r_1$  is the radius of the iris poles.

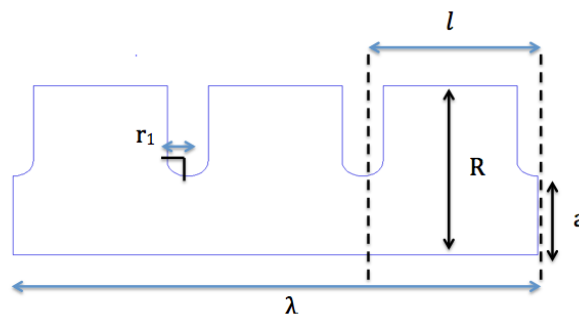


Figure 2: Schematic view of a generic X-band cavity.

In this example we show a configuration for a  $2\pi/3$  TW structure.

### Decelerating Cavity

Here we choose to use a  $2\pi/3$  mode TW X-band structure with parameters given in Table 2 and as computed by the design code SUPERFISH [5].

As we plan on passing through the structure a fairly high current beam we must concern ourselves with HOM effects, thus the optimal tends to larger iris dimensions at the expense of shunt impedance [4]. Figure 3 shows the loss parameter  $k$  as a function of the iris radius.

$$k = \frac{\omega R_s}{4Q}$$

where  $\omega$  is the angular frequency of the RF,  $Q$  is the unloaded quality factor of the structure and  $R_s$  is the cavity shunt impedance. Clearly a larger iris is desired. This is OK as we found in our earlier paper that even for moderate shunt impedance the structure is relatively short as we are limited by the maximum amount of energy we can remove from the drive beam. Based on our previous study the length of this cavity should be 15.3 cm in order to decelerate the beam from 6 MeV down to 1 MeV. Under such conditions the net X-band rf power that can be generated is 1.4 MW.

Figure 4 shows the power dissipated in the cavity walls as a function of the iris radius. As can be seen this is small compared to the available power generated even for larger values of  $a/\lambda$  and so is not a significant factor.

The resulting X-band power is then coupled out of the cavity and transferred to the accelerating structure.

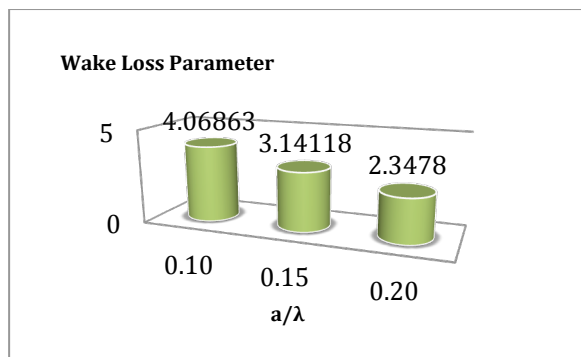


Figure 3: Wake loss parameter vs.  $a/\lambda$ .

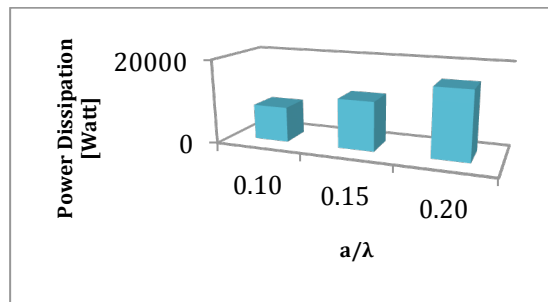


Figure 4: Power dissipation vs.  $a/\lambda$ .

As this structure is powered in a global fashion via the electron beam there is no need to complicate the design with a constant gradient design. Rather we choose a simple constant impedance device.

Figure 5 shows the cavity fields, both electric and magnetic, as computed by SUPERFISH for both Neumann and Dirichlet boundary conditions as specified at the end walls.

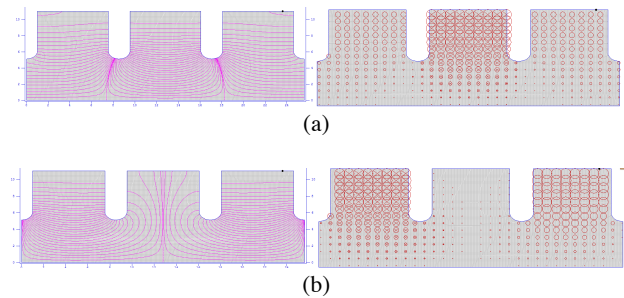


Figure 5: Electric and magnetic field patterns for  $a/\lambda = 0.2$  in (a) Neumann boundary condition at end walls for  $2\pi/3$  mode (b) Dirichlet boundary condition at end walls for  $2\pi/3$  mode.

Table 2: Parameters for Decelerating Cavity

$a/\lambda$	0.2
Phase Advance per cell ( $\psi$ )	$2\pi/3$ radian
Iris radius (a)	0.00512466 m
Cavity Radius (R)	0.0110955 m
Disk Thickness ( $h=2r_1$ )	0.002 m
Quality factor	6456
Length	0.153 m
Frequency	11.7 GHz
Shunt impedance	79.15 MΩ
Power Dissipation	8360.779

### Accelerating Cavity

The optimization for the accelerating cavities follows a different path. This cavity will see a single, relatively low charge pulse, so the aperture requirements are not as severe. Further we wish to maximize the overall integrated voltage seen by the beam during its passage. This clearly argues for high shunt impedance and as long a structure as reasonable.

Our L-band system is also capable of generating beam for over  $10 \mu s$ , i.e. significantly longer than the fill time of typical X-band structures. We will therefore operate the L-band system with shorter pulses, but pulses long enough to completely fill the X-band structure. This then argues for a structure with a very slow group velocity as it will allow us to fill a longer cavity and capitalize on the long L-band rf pulses.

All structure parameters for the TW accelerator can be deduced from those of the SW structure. In particular, the group velocity can be computed by

$$v_g = \frac{d\omega}{dk_z} = \frac{2(2.405)c}{3\pi J_1^2(2.405)} \left(\frac{a}{R}\right)^2 \sin \psi e^{-\alpha h}$$

where  $\psi$  is the phase advance per cavity traveling wave and  $\alpha$  is the attenuation per unit length of the field for the  $TM_{010}$  mode through an iris of wall thickness  $h$ .

If we wish to decrease the group velocity and we have chosen a minimum  $a$ , we are left only with  $\psi$  as a variable. This then argues for a large TW mode number defined as  $n$  in  $2\pi/n$ . This is shown in Figure 6 where the relative velocity coming from the sine term is plotted vs.  $n$ . A value of  $n$  equal to 2 is the SW  $\pi$ -mode. This certainly would argue that the  $2\pi/3$ -mode is not the best choice and that a mode number of more like 15 or 16 would be better and might still be practical.

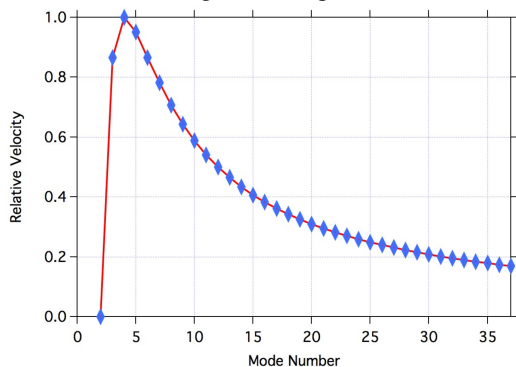


Figure 6: Relative velocity vs. mode number.

For that purpose moving the RF phase advance to  $5\pi/6$  (for  $a/\lambda = 0.1$ ) and using a longer cell length compared to that of the  $2\pi/3$  (for  $a/\lambda = 0.15$ ) mode in order to preserve synchronous acceleration of the electron bunch slows down the group velocity to 0.95%  $c$  and increases  $\alpha_0$  to 1.69 from its  $2\pi/3$  value of 0.30 allowing more efficient deposition of the RF power in the accelerating structure [6,7]. Table 3 shows the parameters of this accelerator structure.

Table 3: Parameters for Accelerating Cavity

$a/\lambda$	0.15	0.1
Inner radius	0.00512466 m	0.00256233 m
Phase Advance	$2\pi/3$ radians	$5\pi/6$ radians
Cavity Radius	0.0110955 m	0.00999 m
Disk Thickness	0.002 m	0.002 m
Frequency [GHz]	11.7 GHz	11.7 GHz
Quality factor	6456	7474
Shunt impedance	79.15 M $\Omega$	185.67 M $\Omega$
Group Velocity	6.38 %	0.95 %

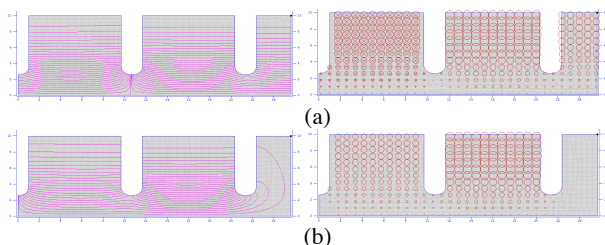


Figure 7: Electric and magnetic field patterns for  $a/\lambda = 0.1$  in (a) Neumann boundary condition for  $5\pi/6$  mode (b) Dirichlet boundary condition for  $5\pi/6$  mode.

Figure 7 shows the cavity fields, both electric and magnetic, as computed by SUPERFISH for both Neumann and Dirichlet boundary conditions as specified at the end walls for the accelerating cavity.

### DISCUSSION AND CONCLUSION

In this study we provide designs for two different TW X-band structures that would allow us to achieve higher energies in a compact way. To achieve higher potential one really needs to extract the X-band power from the X-band decelerating cavity and transfer it to a low group velocity traveling wave structure. Optimizing the group velocity by adjusting the inner radius of the constant-impedance structure and using a more relevant mode both improves the power efficiency and overall integrated potential.

### ACKNOWLEDGMENT

We wish to thank the SLAC National Laboratory Facility for their support and funding and in particular the input from C. Adolphsen. Finally, we wish to thank the senior management of CSU for their support of the accelerator laboratory and accelerator education.

### REFERENCES

- [1] S. G. Biedron, T. Bureson, C. Carrico, A. Dong, J. Edelen, C. Hall, K. Horovitz, S.V. Milton, A. Morin, L. Rand, N. Sipahi, T. Sipahi, P. van der Slot, H. Yehudah, "The CSU Accelerator And FEL Facility", FEL'12, Nara (2012).
- [2] S. G. Biedron, S.V. Milton, N. Sipahi, T. Sipahi, C. Adolphsen, "Passively Driving X-band Structure to Achieving Higher Beam Energies", IPAC 2013, Shanghai, China, May 12-17, 2013.
- [3] N. Sipahi, T. Sipahi, S. V. Milton, S. G. Biedron, "X-band RF power Generation via L-band Accelerator System and Uses" NAPAC 2013, Pasadena (2013) (to be published).
- [4] J. W. Wang, RF Properties Structures of Periodic For Linear Accelerating Colliders\*, SLAC-339, UC-28 (A), Stanford Linear Accelerator Center, Stanford University, Stanford, California, Ph. D. Dissertation (1989).
- [5] J. Warren, et al., "POISSON/SUPERFISH Reference Manual," Los Alamos National Laboratory report LA-UR-87-126 (1987).
- [6] C. Christou, "X-band Linac Technology for a High Repetition Rate Light Source", Nuclear Instruments and Methods in Physics Research A 657, p. 13-21 (2011).
- [7] G. Burt, P.K. Ambattu, A.C. Dexter, T. Abram, V. Dolgashev, S. Tantawi, R.M. Jones, "X-Band Crab Cavities For The Clic Beam Delivery System", 44th ICFA Advanced Beam Dynamics Workshop: X-Band RF Structure and Beam Dynamics, Warrington, United Kingdom, December, 2008.